On the load impact of dynamic wind farm wake mixing strategies

Frederik, Joeri A.; van Wingerden, Jan Willem

DOI
10.1016/j.renene.2022.05.110

Publication date
2022

Document Version
Final published version

Published in
Renewable Energy

Renewable Energy 194 (2022) 582–595

Contents lists available at ScienceDirect

Renewable Energy

journal homepage: www.elsevier.com/locate/renene

On the load impact of dynamic wind farm wake mixing strategies

Joeri A. Frederik , Jan-Willem van Wingerden *

Delft University of Technology, Mekelweg 2, 2826CD, Delft, the Netherlands

ARTICLE INFO

Article history:
Received 4 August 2021
Received in revised form
24 April 2022
Accepted 18 May 2022
Available online 28 May 2022

Keywords:
Dynamic wake mixing
Wind farm control
Damage equivalent load
Blade bearing damage
Dynamic induction control
Individual pitch control
Helix approach

ABSTRACT

In recent studies, the effectiveness of different so-called wake mixing strategies has been assessed in terms of wind farm power maximization. These studies show that by dynamically varying the pitch angles of a wind turbine, wake mixing can be enhanced to increase the overall power production of a wind farm. However, such strategies also increase the loads experienced by the turbine, which may disqualify such methods as viable wind farm control strategies. In this paper, an extensive analysis of the load effects of two specific wake mixing strategies, Dynamic Induction Control (DIC) and the helix approach, is presented. The damage equivalent load of critical components such as the turbine blades and tower is assessed, and the risk of fatigue damage on the blade pitch bearings is determined. This paper therefore contributes to determining the implementability of such wake mixing strategies in wind farms of the future.

1. Introduction

Renewable energy sources are projected to account for an increasingly large amount of the total energy demand [1]. By 2050, wind energy alone is expected to generate approximately one third of the world's electricity [2]. A large portion of this capacity should be generated in offshore wind farms. In the Netherlands, the government plans to increase its offshore wind capacity, which is currently 1 GW, to 11.5 GW by 2030, by building six large wind farms in the Dutch North Sea [3].

Placing wind turbines together in wind farms offers significant, mostly economical advantages compared to individual wind turbines [4]. Mainly, construction and maintenance costs are lower, and a smaller surface area is necessary to generate a certain amount of power. However, there are also disadvantages associated with the operation of wind turbines in wind farms. An operating wind turbine induces a wake, a region behind the turbine in which the wind speed is lower and the turbulence higher. Consequently, a turbine that is located in this region generates less power and experiences higher structural loads.

This interaction between turbines in a wind farm, induced by the wakes of turbines, poses an interesting control problem. The control actions implemented on an upstream turbine influence not only the performance of this turbine, but also that of the turbines in its wake. As a result, optimizing the performance of a wind farm as a whole is not as easy as finding the optimal control actions for all individual turbines. Control methodologies can improve the performance of wind farms by increasing the overall power generated, or by decreasing the overall Damage Equivalent Loads (DELs). These two objectives often conflict, as improving the energy capture generally leads to worse load behaviour, and vice versa.

Over the years, many different control strategies that maximize the power production of wind farms have been investigated. The two most popular methods in literature are derating control and wake redirection control. In derating control, the power generation of upstream turbines is derated, for example by means of changing the blade pitch angles or the generator torque (see, e.g., Refs. [5,6]). This leads to a lower wake deficit, such that downstream turbines can increase their energy capture. However, more recent studies have shown that the benefit of derating is in practise small to non-existing [7,8].

Wake redirection control usually utilizes a different control degree of freedom of wind turbines: the angle of the rotor with respect to the wind, which is called the yaw angle. By creating a yaw offset with respect to the wind direction, the wake of a turbine can be redirected away from downstream turbines [9]. Similar to derating control, this leads to a lower than optimal power production of the controlled turbine, but increased energy capture of

* Corresponding author.
E-mail address: j.w.vanwingerden@tudelft.nl (J.-W. van Wingerden).

https://doi.org/10.1016/j.renene.2022.05.110

downstream machines. This strategy has shown promising results both in scaled wind tunnel experiments [10,11] and field tests [12–14].

Until recently, the research on wind farm control for power maximization focused primarily on finding the *steady state* optimum: as long as the operating conditions stay the same, the control input, either the derating factor or the yaw angle, is kept constant. However, a broader approach to this control problem is to consider all dynamical signals. In Ref. [15], Model Predictive Control is used to find the optimal dynamical thrust coefficient of each turbine in a wind farm. Although this approach is complex and computationally expensive, the potential gain is shown to be significant.

The findings presented in Ref. [15] has led to an increasing amount of research into the topic of dynamic control for wind farm power maximization. In Ref. [16], a more practically implementable approach to this Dynamic Induction Control (DIC) is suggested where the thrust factor of upstream turbines is varied sinusoidally. This approach has been validated in wind tunnel experiments in Ref. [17]. A different strategy that uses dynamic yawing is investigated in Refs. [18,19]. Finally [20], presents the *helix approach*, which uses dynamic pitching of the individual blades to obtain the same effect without large variations on the rotor thrust.

It is hypothesized in Ref. [20] that, due to the much lower variations in rotor thrust, the DELs are also lower compared to DIC. In this paper, this hypothesis is tested by studying the blade and tower bending moments when different control strategies are applied. These moments are obtained from the FAST wind turbine simulator [21,22] and compared to the results obtained from the flow simulation code called SOWFA [23]. The load data from both models are assessed and compared to evaluate the effect of the different dynamic control strategies on the lifetime of turbines.

This paper is structured as follows: in Section 2, the FAST and SOWFA simulation environments are described, followed by the research methodology to obtain turbine load signals in Section 3. Section 4 discusses the different dynamic control approaches and how they are implemented. In Section 5, the results of the simulations are presented, followed by the conclusions in Section 6.

2. Simulation environment

In this section, the simulation environments FAST and SOWFA are described, and relevant literature is presented. These tools are used to obtain the load performance of wind turbines in a wind farm that applies dynamic control. Finally, the different simulation cases and relevant signals that are used in Section 3 to determine the turbine loads are described.

2.1. FAST turbine model

For the single turbine simulations, an NREL 5 MW reference turbine [24] is used in the OpenFAST tool [21], based on the FAST v8 code [22]. The FAST turbine model is coupled with MATLAB-Simulink to enable the implementation of different control strategies.

Experiments with different wind speeds are executed to grasp the full range of operating conditions that a turbine experiences. The cut-in, rated and cut-out wind speeds of a NREL 5 MW turbine are 3 ms^{-1}, 11.4 ms^{-1}, and 25 ms^{-1}, respectively. However, dynamic wake mixing strategies are mainly aimed at the below-rated regime, as the power loss of downstream turbines in the above-rated regime is significantly lower. Subsequently, the power gain obtainable at downstream turbines by means of wake mixing is lower in this regime. Nonetheless, from an academic point of view, it is still interesting to investigate all operating regimes of the turbine. Therefore, simulations have been executed with an average effective wind speed ranging from 6 ms^{-1}–15 ms^{-1}.

For the experiments shown in this paper, turbulent wind profiles according to the Normal Turbulence Model (NTM) are used [25]. Two different TI conditions are evaluated:

- A *low-TI* case with a turbulence intensity of approximately 5%. These conditions are comparable to the operating conditions in Refs. [20,26] and the SOWFA flow simulations presented here. This case therefore enables a comparison between FAST and SOWFA, and can serve to validate the results obtained in the latter.
- A *high-TI* case, according to the *IEC Class A*, with an average TI of 16% [27]. These conditions are identical to the simulations executed in Ref. [17], where the load effects of DIC are evaluated using a different turbine model. This case therefore serves as validation of these earlier results, while including a comparison with the novel helix approach.

FAST produces 40 different turbine outputs, such as time, rotor azimuth, pitch angle and generator power. To determine the lifetime, the Blade root moments In-Plane (IP) and Blade root moments Out-of-Plane (OoP) are used. These are defined in the fixed (rotor) frame, i.e., the frame of the wind turbine. Note that, when the pitch angles are known, these moments can be transformed into the flapwise and edgewise moments, which are defined in the frame of the blades, as follows:

$$\begin{aligned} M_{\text{flap}} &= M_{\text{OoP}}\cos(\theta) + M_{\text{IP}}\sin(\theta) \\ M_{\text{edge}} &= M_{\text{OoP}}\sin(\theta) + M_{\text{IP}}\cos(\theta), \end{aligned} \tag{1}$$

where θ is the blade pitch angle. From these equations, it follows that for pitch angles close to zero degrees, the OoP and the flapwise bending moments are more or less equivalent, as are the IP and edgewise moments. In this paper, only the OoP and IP bending moments are therefore evaluated. Of these two signals, the OoP moment is the most relevant: it can be shown that the IP moments are barely affected by the different control strategies, as gravity is the determinant force causing these moments.

Apart from the blade loads, the tower base bending moments in fore-aft and side-side direction can also be extracted from FAST and evaluated [22]. Again, the fore-aft moment is the most interesting of the two signals, as this load is directly affected by the varying thrust force induced by the wake mixing strategies. Finally, the pitch bearing damage is evaluated based on the pitch action and the blade moments.

2.2. SOWFA simulation environment

The effectiveness of the proposed dynamic control strategies have been evaluated in the Simulator fOr Wind Farm Aplications (SOWFA, see Ref. [23]). SOWFA is a high-fidelity flow simulation environment that uses Large-Eddy Simulations (LES) for fluid dynamics in a turbulent atmosphere. In the experiments shown in this paper, turbines are modeled in SOWFA using the Actuator Line Model (ALM), see Ref. [28].

SOWFA is an extremely powerful tool to evaluate the performance of wind farm controllers with high fidelity. However, it also requires a substantial amount of computational power. Even using High Performance Computing (HPC), a single simulation can take more than a week to complete. Subsequently, it is not feasible to execute the wide range of simulations performed in FAST. Instead, the different control strategies are evaluated in one single operating case. The selected case is identical to the one presented in Ref. [26]. This paper shows that the wake mixing strategies are effective in terms of increasing power generation, which makes the evaluation of the loads in these conditions relevant.

Realistic wind inflow profiles are created in SOWFA by running so-called precursor simulations with a neutral Atmospheric Boundary Layer (ABL). A below-rated inflow wind speed of 8 ms^{-1} with a turbulence intensity of 5% is implemented. A similar control architecture is used as in FAST: a *K-omega-squared* torque controller is employed, while the baseline pitch control keeps the blade pitch angles at the steady-state optimal C_P. The dynamic pitch controllers are superimposed on this baseline control output.

The performance of the wake mixing algorithms that are being tested in this paper lies in the interaction between upstream and downstream turbines. However, this interaction also affects the loads experienced by downstream machines. Therefore, analyzing the loads of the upstream turbine does suffice to determine the full effect of these algorithms on a wind farm. In FAST, it would only be possible to execute this analysis of a downstream turbine if the flow field in the wake is known, which is not a straightforward task. In SOWFA, however, it is relatively simple to implement more than one wind turbine. It is therefore also possible to assess the performance of a turbine located in the wake of the controlled turbine. To facilitate this analysis, the wake mixing strategies are also tested in SOWFA on a small wind farm of two turbines. The downstream turbines is located 5 turbine diameters ($5D$) behind the upstream turbine, aligned with the wind, and is controlled using the baseline greedy control strategy (see Section!4). This turbine thus fully experiences the wake behaviour caused by the control strategies implemented on the upstream machine. As a result, the most important load effects of these approaches on the entire wind farm can be evaluated.

As SOWFA is a high-fidelity *flow* simulator, with relatively simple turbine models, the turbine data obtained from SOWFA can be considered less reliable than that of the specific turbine model from FAST. The load data of an upstream turbine in SOWFA is therefore first compared to the results obtained in FAST to assess its reliability, and used to estimate the loads on a downstream turbine. To enable this comparison, an ALM model of the NREL 5 MW turbine is implemented in SOWFA. The blades is divided into 40 sections, and the forces acting on these sections can be extracted. The root bending moments acting on the blades can then be determined by the simple momentum equation $M = rF$, with r the distance of the center of mass of each blade element to the blade root. A summation of all blade element moments results in the moment acting on the blade root.

The tower fore-aft bending moment is determined by the addition of two individual signals: the drag force of the wind acting on the tower, and the rotor thrust. Of these two, the rotor thrust is the dominant force, as it is larger and experiences more fluctuations than the tower drag force. Finally, an assessment of the pitch bearings is executed by using the blade loads and pitch actuation signals.

It should be noted that an effort has been made to make the wind profiles in both simulation environments comparable, but that further efforts are needed to truly achieve comparable wind profiles. However, the goal of this paper is not to present an optimized comparison between FAST and SOWFA. The main contribution of the SOWFA simulations is that it enables an evaluation of the loads on a downstream turbine, which would not be achievable in FAST.

3. Methodology

This section elaborates on the research methodology used to estimate the impact of the wake mixing strategies described in Section 4 on the lifetime of turbines. This methodology entails two parts: first, the principles behind Damage Equivalent Load (DEL) are described in Section 3.1. Then, Section 3.2 evaluates how to assess the effects of increased pitch actuation on the bearings.

3.1. Damage equivalent load

A common method used in literature (see, e.g., Refs. [29–31]) to quantify the amount of damage caused by the load on a certain element, is called the Damage Equivalent Load (DEL). This approach uses the rainflow counting algorithm to determine the number of oscillation cycles and their amplitude in the load signal. Based on these cycles, the DEL can be calculated using [32]:

$$S = \left(\frac{\sum_{i=1}^{n} (\Delta S_i)^m N_i}{N} \right)^{1/m}, \tag{2}$$

where S is the DEL, ΔS_i the amplitude of cycle i, with n the total number of cycles. N_i is the number of cycles with that specific amplitude, and m is the inverse of the material Wöhler slope. N is the reference number of cycles, taken as 1 here. The inverse Wöhler slope is given in Table 1 for different materials. Note that the effect of this coefficient mainly affects the absolute value of the DEL, and has little to no effect on the relative results between different simulations. Subsequently, the results shown in Section 5 assume an inverse Wöhler coefficient of $m = 10$ for the blades.

3.2. Pitch bearing damage

The control strategies described in Section 4 require pitch action to enhance wake mixing. Naturally, increasing the pitch demand also increases the likelihood of damage to the pitch bearings. However, unlike the bending moments affecting the blades and tower of a turbine, the damage caused by pitching a blade is harder to capture in a single equation. Damage to the bearings of turbine blades is induced by a combination of signals: the rotation of the blade, the amplitude of the rotation, and the force exerted on the blade. This section aims to describe the method used to indicate the magnitude with which the pitch bearing damage increases and is based on the methods presented in Refs. [33,34].

In general, damage in pitch bearings is caused by either Rolling Contact Fatigue (RCF) or Surface-Induced Damage (SID) [35]. In Ref. [33], it is shown that RCF occurs mostly due to long, steady rotations, whereas SID is caused by oscillations with a smaller amplitude. The pitch action that is implemented on a turbine with the dynamic strategies investigated in this study, are all oscillations with a relatively low amplitude of $\pm$ 2.5°. It can therefore be concluded that surface-induced damage is the most likely to occur here.

A number of parameters influence the risk and severity of SID occurring: the amplitude and speed of the oscillations, the load, and the lubricant used in the bearing [33]. An oscillation with a smaller amplitude is more likely to cause damage, since the forces are acting on a smaller surface area of the bearing. To analyse the likelihood of damage occurring, it is therefore necessary to first determine the amplitude and mean of the different oscillations. Furthermore, the number of cycles and the associated operation time is important to detect potential damage: a cycle that occurs more often is much more likely to result in bearing damage.

Table 1
The inverse Wöhler slope m for the wind turbine materials.

Material	Component	m
Welded steel	Tower	4
Glass fiber	Blade	10
Carbon fiber	Blade	14

For fatigue analysis, such as the DEL method presented in Section 3.1, the rainflow counting algorithm is commonly used to distinguish load cycles. However, for SID to bearings, every interruption of a movement has to be taken into account [33]. For this purpose, rainflow counting overestimates the number of cycles with a smaller amplitude (see the cycles 3 and 5 in Fig. 1), as well as the amplitude of longer cycles (see cycle 1 in Fig. 1). An alternative that is more suitable to evaluate bearing damage is range-pair counting [33], where every change of direction indicates the beginning of a new cycle. Note that with a strictly sinusoidal signal with a single frequency, both methods yield the same result.

In this paper, the range-pair counting algorithm is implemented to determine the number of cycles with different amplitudes. For the most frequent cycles, the results are binned based on the average pitch angle to determine where SID is most likely to occur. Finally, the resulting bending moments are binned to determine the load on the bearing for these critical oscillations.

To give an overview of risk of blade bearing damage occurring under different operating conditions, three different cases are assessed. First, the low TI case described in Section 2 is used, with an average inflow wind speed of 8 ms^{-1}. This case represents the conditions in which wake mixing strategies are the most effective, as the power deficit of a downstream turbine is the most significant in these conditions. Secondly, the high TI case is assessed, both in below-rated (8 ms^{-1}) and an above-rated (14 ms^{-1}) wind speeds. Especially in above-rated wind speeds, wake mixing strategies are less effective, while the pitch actuation and blade loads increase. It is therefore questionable whether these strategies should be implemented under these conditions. For the sake of completeness, the more extreme stresses present in this simulation case are evaluated nonetheless.

4. Control strategy

In this section, the control strategies implemented on the turbine models in FAST and SOWFA are described. Four different control strategies have been implemented in FAST, all using a similar control framework. These different control strategies are:

- *Baseline case*, where the turbine is controlled for optimal (steady-state) power extraction;
- *Dynamic Induction Control* (DIC), where a low-frequent sinusoidal reference is superimposed on the baseline collective pitch angle;
- *Helix* Dynamic Individual Pitch Control (DIPC), as proposed in Ref. [20]. Both the counterclockwise (CCW) and clockwise (CW) rotating helices are investigated;
- *Individual Pitch Control* (IPC), where the individual blade pitch capabilities are used to minimize periodic loads on the blades.

Since the Helix approach is applied in clockwise and counterclockwise rotational direction, this gives a total of 5 control cases. All the investigated control strategies are superimposed on the baseline controller, as shown in Fig. 2. In the baseline case, a standard *K-omega-squared* torque control is implemented in the below-rated regime [36,37], while the blade pitch angles are kept constant at the optimal power coefficient C_P to ensure maximal power generation. In the above-rated regime (i.e., when the wind speed exceeds 11.4 ms^{-1}), the torque is kept constant while the collective pitch angles are controlled to ensure rated power production. Both dynamic induction control and the helix approach use only the pitch angles of the turbine, while the torque controller is kept in place. The pitch control for these strategies is superimposed on the baseline pitch controller.

To decrease the structural loads of turbines, and of turbines blades specifically, Individual Pitch Control (IPC) is a well-known and established methodology. IPC for load mitigation was first proposed in Ref. [29], and has received a large amount of interest since. The concept is the following: by pitching the blades of a turbine independently, the periodic variations in moments experienced by these blades can be reduced significantly with minimal impact on the power production. The conventional approach to IPC as proposed in Refs. [29,38] uses the MBC transformations [39]:

$$\underbrace{\begin{bmatrix} M_0(t) \\ M_{\text{tilt}}(t) \\ M_{\text{yaw}}(t) \end{bmatrix}}_{M_T(t)} = \underbrace{\frac{2}{3}\begin{bmatrix} 0.5 & 0.5 & 0.5 \\ \cos(\psi_1) & \cos(\psi_2) & \cos(\psi_3) \\ \sin(\psi_1) & \sin(\psi_2) & \sin(\psi_3) \end{bmatrix}}_{\mathbf{T}(\psi)} \underbrace{\begin{bmatrix} M_1(t) \\ M_2(t) \\ M_3(t) \end{bmatrix}}_{M(t)}, \quad (3)$$

where $M_0(t)$, $M_{\text{tilt}}(t)$ and $M_{\text{yaw}}(t)$ are the cumulative out-of-plane rotor moment, the tilt moment and the yaw moment, respectively. $\mathbf{T}(\psi)$ is the transformation matrix as a function of blade azimuth angle $\psi = [\psi_1\ \psi_2\ \psi_3]^T$, and $M(t)$ are the measured blade out-of-plane bending moments.

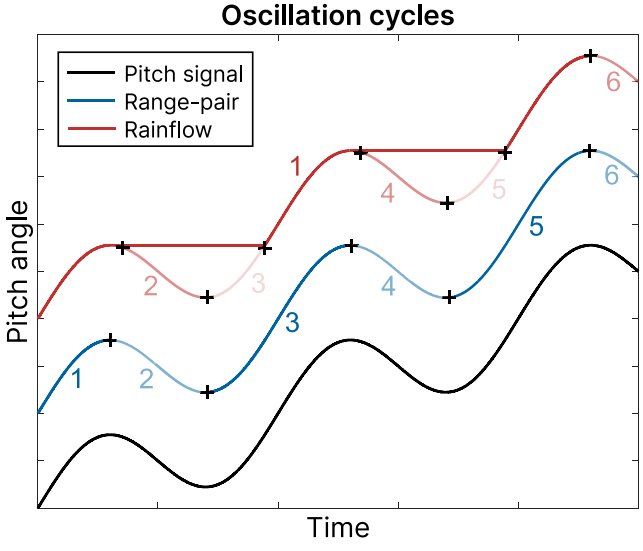

Fig. 1. Visualization of the difference between rainflow and range-pair counting. In black, the original oscillating signal is shown. The blue line shows the cycles identified by range-pair counting, while the red line represents the cycles obtained with rainflow counting. The crosses indicate where one cycle ends and the next one starts.

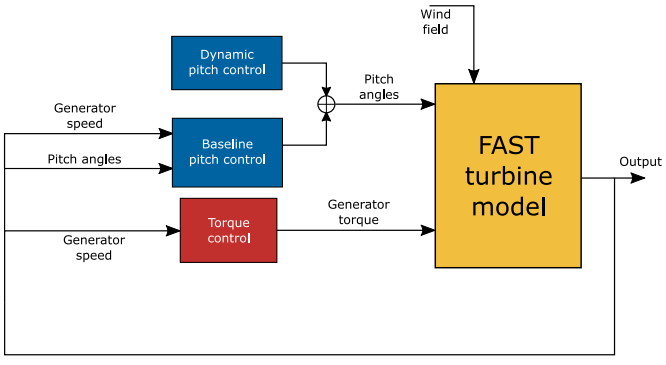

Fig. 2. Control diagram of the wind turbine model in FAST. The baseline pitch and torque control are designed to maximize steady-state power generation. The different dynamic pitch control strategies are superimposed on the baseline control action, while the baseline torque control remains unchanged.

The MBC transformation projects the original blade moments $M(t)$ onto a non-rotating frame $M_T(t)$. The once-per-rotation (1P) moments appear as a constant tilt and yaw moment in this non-rotating frame, and by implementing simple PI-controllers, these moments can be regulated to zero by means of the tilt angle θ_{tilt} and yaw angle θ_{yaw}. The individual blade pitch angles can then be found by using the inverse transformation

$$\underbrace{\begin{bmatrix}\theta_1(t)\\ \theta_2(t)\\ \theta_3(t)\end{bmatrix}}_{\theta(t)} = \underbrace{\begin{bmatrix}1 & \cos(\psi_1) & \sin(\psi_1)\\ 1 & \cos(\psi_2) & \sin(\psi_2)\\ 1 & \cos(\psi_3) & \sin(\psi_3)\end{bmatrix}}_{\mathbf{T}^{-1}(\psi)} \underbrace{\begin{bmatrix}\theta_0(t)\\ \theta_{\text{tilt}}(t)\\ \theta_{\text{yaw}}(t)\end{bmatrix}}_{\theta_T(t)}, \tag{4}$$

where the cumulative pitch angle θ_0 is usually set to 0. By applying the pitch angles $\theta(t)$ thus obtained, the 1P blade loads, often the most dominant, can be removed from the spectrum [38,40]. This results in significantly lower turbine Damage Equivalent Loads (DELs). The only disadvantage that needs to be considered with IPC is the substantial increase in pitch actuation, which can be up to a factor 3 bigger in above-rated conditions [38]. Fig. 3 presents the control implementation of this controller, where the integrator gain of the PI controller is set to $5 \cdot 10^{-6}$. In this paper, this conventional IPC approach is used as a comparison case for the wake mixing strategies in terms of pitch bearing damage.

With Dynamic Induction Control (DIC), the thrust factor of an upstream wind turbine is varied over time in order to enhance wake mixing. Subsequently, the wind speed in the wake is increased and the energy capture of a potential downstream turbine is increased. This strategy was first proposed in Ref. [15]. In this study, the thrust factor of the turbines is optimized over a receding horizon using adjoint-based optimization. This approach results in a significant increase in wind farm energy capture, but does involve a couple of complications that make practical implementability infeasible. First of all, the computation time of the optimization algorithm used far exceeded the horizon of the found control solution. As a result, real-time implementation of this approach is not possible. Secondly, the thrust factor was used as a control input, while in reality this parameter is not directly controllable: it depends on many different signals, such as the wind speed, rotor speed, blade pitch angles and generator torque.

By limiting the time-varying thrust factor to periodic signals, the first of these two complications is resolved [16]. In this study, a grid search is performed to find the optimal frequency of excitation for an upstream turbine, in the case of a wind farm with 4 aligned turbines. This frequency is scaled for the wind speed and rotor diameter, resulting in the dimensionless Strouhal number St:

$$St = \frac{fD}{U}, \tag{5}$$

where f is the excitation frequency, D the rotor diameter and U the undisturbed inflowing wind velocity. In Ref. [16], an optimal Strouhal number of $St = 0.25$ is reported. Note that this results in a very low frequency: for the NREL 5 MW turbine operating at a wind speed of 8 ms^{-1}, the excitation period would be 63 s.

The strategy of periodic excitations is also implemented successfully in scaled wind tunnel experiments [20]. To resolve the second complication mentioned above, a time-varying thrust force is achieved by prescribing a periodic variation of the collective blade pitch angles. Although a sinusoidal pitch signal does not directly result in a sinusoidal thrust force, it is shown that the wind farm power generation can also be increased by following this approach. As the collective pitch angle of a wind turbine, unlike the thrust force, is directly controllable, this procedure is also followed in this paper.

An alternative to DIC is proposed in Ref. [20]: instead of varying the *collective* pitch of an upwind turbine, the *individual* pitch angles can be used to induce wake mixing. Unlike DIC, the proposed method does not aim to apply a periodic variation on the thrust force, but the *moments* acting on the rotor disk. The tilt moment (in vertical direction) and yaw moment (in horizontal direction) can be found by applying the Multi-Blade Coordinate (MBC) transformation that is also used in classical IPC, see Equation (3).

A desired tilt and yaw moment can be achieved by prescribing a corresponding tilt and yaw angle (Equation (4)). By imposing a moment on the rotor disk, the direction of the wake can be manipulated in vertical or horizontal direction, respectively. It is shown in Ref. [41] that, when applied statically, this effect is very small. However, when these moments are varied over time, the impact on the wake is significant enough to enhance wake mixing similar to DIC. It is therefore proposed in Ref. [20] to impose a low-frequency periodic signal on the tilt and yaw moments of an upwind turbine. It is shown that, when these signals are given a 90° phase offset, the resulting pitch frequency becomes $f_r \pm f_e$, where f_r is the rotational frequency and f_e the excitation frequency of the tilt and yaw moments. As $f_r \gg f_e$, typically by a factor 10, the blade pitch frequency of this method is close to the once-per-rotation (1P) frequency typically used in IPC for load mitigation.

When these individual blade pitch angles are implemented on a wind turbine, the resulting wake is displaced alternately in vertical and horizontal direction. This causes a rotation in the wake that gives it a helical shape. Subsequently, this strategy is called the *helix approach* in Ref. [20]. Depending on whether the tilt moment has a phase lead or lag with respect to the yaw moment, this helix rotates in clockwise or counterclockwise direction, respectively.

Simulations in SOWFA have shown that the helix approach, especially in counterclockwise direction, is equally effective in enhancing wake mixing for wind farm power maximization. It is hypothesized in Ref. [20] that the helix approach could result in lower structural loads for the controlled turbine, as the variations in thrust force associated with DIC are not present. However, the helix approach also requires significantly more pitch actuation, as visualized in Fig. 4. Subsequently, the blades and pitch bearings might experience increased structural loads.

In [17], the structural loads of a turbine operating with DIC are investigated in the aero-elastic code Cp-Lambda [42]. In this paper, similar simulations are executed in FAST, for DIC and the helix approach. With these simulations, the hypothesis that the helix

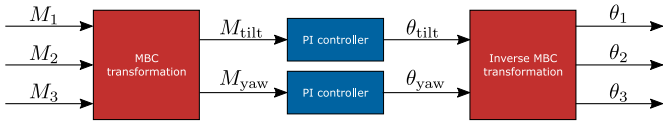

Fig. 3. Block schematic representation of the conventional individual pitch control strategy as implemented in this paper.

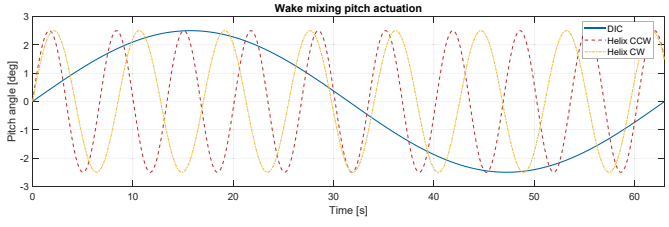

Fig. 4. The pitch actuation of one of the blades of a turbine executing different dynamic control strategies. This example shows the pitch actuation for the NREL 5 MW turbine operating at a wind speed of 8 ms^{-1} and with a Strouhal number of $St = 0.25$.

approach is a lower-loads wake mixing alternative for DIC can be tested. Furthermore, the pitch bearing damage is evaluated and compared to IPC for load mitigation, to quantify the impact of increased pitch actuation on the turbine life span.

5. Results

This section describes the results obtained from the different simulations defined in Section 2. First, an analysis of the turbine loads over different wind velocities is performed. Subsequently, the simulations with a wind speed of 8 ms^{-1} and a relatively low Turbulence Intensity (TI), which are executed in both FAST and SOWFA, are compared. Next, an analysis of the loads on a downstream turbine is executed using data from SOWFA. Finally, the pitch bearing damage for the different control strategies is assessed.

5.1. Turbine loads

In this section, the loads on a turbine that is executing different wake mixing strategies are assessed. First, turbine operation at the below-rated wind speed of 8 ms^{-1} is evaluated, followed by an analysis of the turbine Damage Equivalent Load (DEL) over a range of wind speeds from 6 ms^{-1}–15 ms^{-1}. Both the low and the high Turbulence Intensity (TI) simulations, as defined in Section 2, are assessed.

The evolution of the most relevant turbine signals for the different methodologies is shown in Fig. 5. As the average wind speed of 8 ms^{-1} is well below rated, the pitch action comprises solely what is prescribed by the wake mixing controller. Although the periodic excitation of DIC on the rotor thrust is evident, the resulting effect on the generator power is limited: it is still present, but the amplitude is much smaller than on the rotor thrust.

The Power Spectral Densities (PSDs) of the bending moments are shown in Fig. 6. In the blade bending moments, the pitch frequency is clearly visible for all wake mixing strategies. In the baseline case, the single biggest peak is at the 1P frequency, as would be expected. With DIC, the PSD looks very similar, apart from a sharp peak at the excitation frequency f_e. The same can be said about both helix approaches, where the excitation frequency is the 1P frequency plus or minus f_e for the counterclockwise and clockwise helix, respectively. These peaks are wider than with DIC, since in this case the pitch frequency depends on the varying turbine rotor speed.

The PSD of the tower bending moments shows that in the baseline case, no steep peaks are present, as was the case for the blade moments. Two broader peaks around the tower natural frequency (0.324 Hz) and the 3P frequency are visible. When DIC is applied, a sharp peak at the excitation frequency is observed, as was the case for the blades. Additionally, the amplitude of the PSD around the natural frequency also slightly increases compared to the baseline. It can therefore be concluded that the tower natural frequency is excited by DIC. With the helix approach, this is not the case: around the natural frequency, the PSD is very similar to the baseline case. However, also the helix creates a tower moment at the excitation frequency f_e, as can be seen in the inset of Fig. 6b. Note that, interestingly enough, this is not the pitch frequency of the helix, but rather the frequency with which the yaw and tilt moment vary. This variation evidently also results in a moment on the tower in fore-aft direction, although the amplitude is significantly lower than with DIC.

(a) Blade Moment Out-of-Plane (MOoP) PSD.

(b) Tower PSD.

Fig. 7 shows the turbine DELs for DIC and the helix over different wind speeds and TI's. As expected, these strategies increase the DELs of both the blade Out-of-Plane (OoP) and tower bending moments. Where DIC results in slightly lower blade DELs than the helix, the tower DELs are increased dramatically. The helix on the other hand has only a limited effect on the tower DELs, as this approach does vary the thrust factor of the turbine over time.

The rated wind speed for the NREL 5 MW turbine used in these simulations is 11.4 ms^{-1}. In the below-rated regime, the baseline collective pitch controller keeps the blade angles constant, while above 11.4 ms^{-1}, the collective pitch angles are controlled to guarantee rated power. These different operating regimes are also visible in the results from Fig. 7. At above-rated wind speeds, the DELs no longer increase as the average wind speed increases; in some cases, specifically when DIC is applied in low TI, they even decrease as the wind speed increases. However, wake mixing strategies are more effective in the below-rated regime, and therefore more likely to be applied here. Therefore, the below-rated results should be considered the most relevant.

(a) Blade Out-of-Plane (OoP) DEL.

(b) Tower DEL.

To obtain a comprehensive indicator for the impact of the different strategies on the fatigue loads, the Weibull-weighted

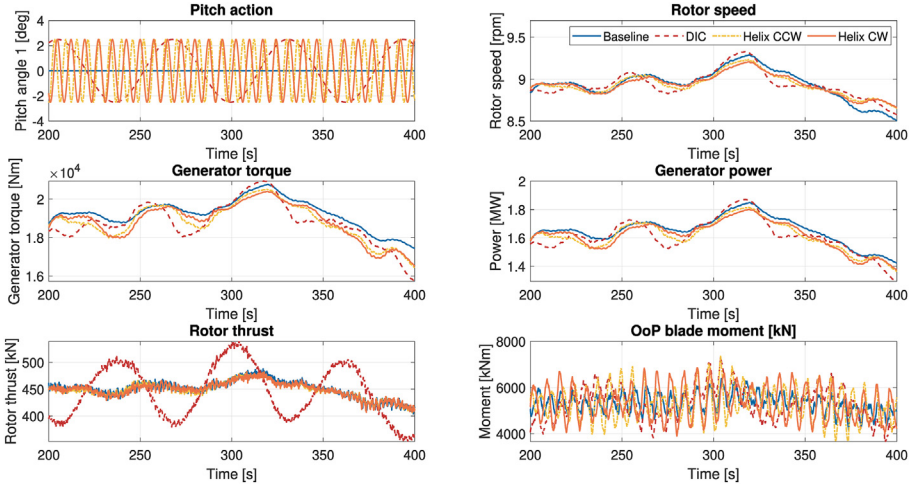

Fig. 5. Time domain behaviour, as simulated in FAST, of the most relevant turbine signals for the baseline case and the different wake mixing approaches, in low TI, below-rated wind conditions.

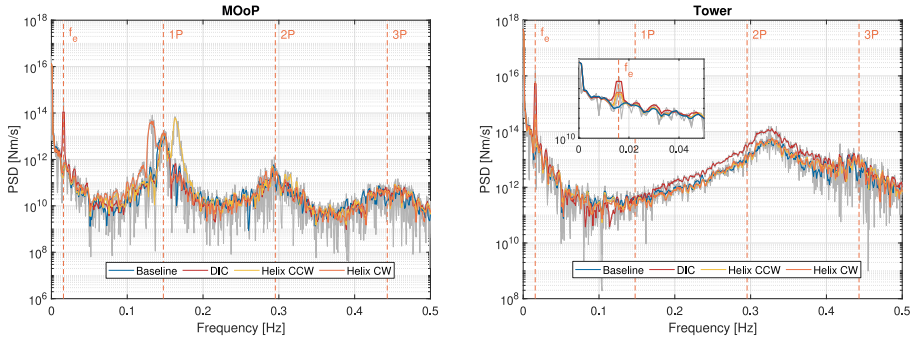

(a) Blade Moment Out-of-Plane (MOoP) PSD. (b) Tower PSD.

Fig. 6. The Power Spectral Density (PSD) for the blade out-of-plane (left) and tower (right) bending moments for the different wake mixing strategies. The results are shown for a wind speed of 8 ms^{-1} and a turbulence intensity of 5%. The results are filtered using a 3-sample moving average filter to obtain smoother signals, the original signals are shown in grey. The inset on the right shows a close-up of the tower loads at the excitation frequency f_e.

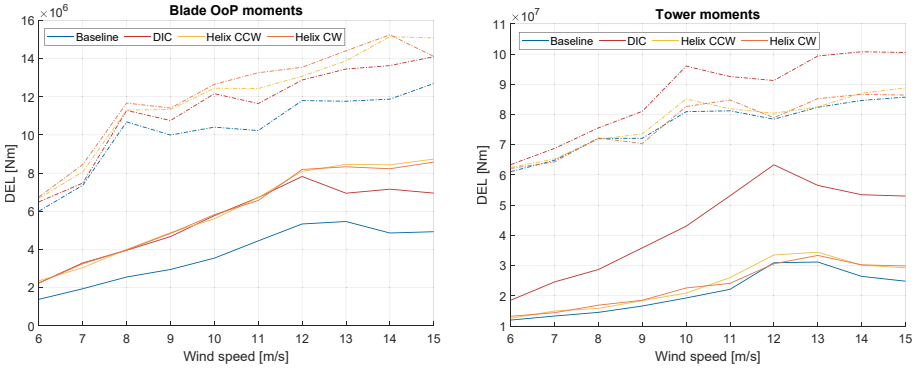

(a) Blade Out-of-Plane (OoP) DEL. (b) Tower DEL.

Fig. 7. The Damage Equivalent Load (DEL) for the blade out-of-plane and tower bending moments for the different wake mixing strategies. The results are shown for different average wind speed simulations with low (solid) and high (dash-dotted) Turbulence Intensity (TI).

DELs, as previously used in Ref. [17], can be considered. This approach combines the DELs from Fig. 7 with the Weibull probability distribution of each particular average wind speed. As such, it gives an accurate estimate of the fatigue loads if the control strategies were to be implemented over the full range of tested wind speeds, all of *IEC Class A* with a TI of 16% [27]. The results of this Weibull-weighted fatigue analysis are shown in Table 2.

This table shows that the weighted results are comparable to the 8 ms^{-1} results shown in Table 4: the fatigue loads on the blades increase significantly for all strategies, while the tower is mostly affected by DIC. In higher turbulence, the loads in the baseline case are significantly higher. As a result, the relative effect of the wake mixing strategies on the fatigue loads is much smaller. However, the general results are the same: significantly higher tower loads for DIC, and slightly higher blade loads for the helix.

Table 2
Weibull-weighted Damage Equivalent Load (DEL) of the wake mixing strategies over the full range of simulations (6–15 ms^{-1}) with low and high Turbulence Intensity (TI). The most significant load increase is colored in red.

Low TI	**Baseline**	**DIC**	**Helix CCW**	**Helix CW**
Blades [Nm]	$3.54 \cdot 10^6$	$5.31 \cdot 10^6$ +50.1%	$5.67 \cdot 10^6$ +60.1%	$5.66 \cdot 10^6$ +59.7%
Tower [Nm]	$2.02 \cdot 10^7$	$4.11 \cdot 10^7$ +103.7%	$2.25 \cdot 10^7$ +11.4%	$2.23 \cdot 10^7$ +10.5%
High TI	**Baseline**	**DIC**	**Helix CCW**	**Helix CW**
Blades [Nm]	$10.0 \cdot 10^6$	$11.1 \cdot 10^6$ +10.4%	$11.6 \cdot 10^6$ +15.4%	$11.8 \cdot 10^6$ +17.9%
Tower [Nm]	$7.52 \cdot 10^7$	$8.51 \cdot 10^7$ +13.1%	$7.67 \cdot 10^7$ +1.9%	$7.62 \cdot 10^7$ +1.2%

Table 3
The free-stream wind characteristics, mean wind speed (WS) and turbulence intensity (TI), in FAST and SOWFA.

Tool	**Mean WS**	**TI**
FAST	8.00 ms^{-1}	4.53%
SOWFA	8.05 ms^{-1}	4.87%

Table 4
Damage Equivalent Load (DEL) comparison between FAST and SOWFA. All percentages shown are relative to the corresponding baseline case. The most significant load increase is colored in red.

	Baseline	**DIC**	**Helix CCW**	**Helix CW**
Blades (FAST) [Nm]	$2.61 \cdot 10^6$	$4.06 \cdot 10^6$ +55.7%	$4.27 \cdot 10^6$ +63.6%	$4.24 \cdot 10^6$ +62.5%
Blades (SOWFA) [Nm]	$2.35 \cdot 10^6$	$5.02 \cdot 10^6$ +114.0%	$4.55 \cdot 10^6$ +94.2%	$4.64 \cdot 10^6$ +97.9%
Tower (FAST) [Nm]	$1.44 \cdot 10^7$	$2.86 \cdot 10^7$ +99.2%	$1.56 \cdot 10^7$ +8.7%	$1.68 \cdot 10^7$ +16.8%
Tower (SOWFA) [Nm]	$1.11 \cdot 10^7$	$2.63 \cdot 10^7$ +138.1%	$1.09 \cdot 10^7$ −1.2%	$1.04 \cdot 10^7$ −6.4%

5.2. Comparison between FAST and SOWFA

In this section, the simulations performed in the turbine model FAST and flow model SOWFA are compared. First of all, the resemblance of the inflow wind conditions in FAST and SOWFA are evaluated. As described in Section 2, both flow fields are created in fundamentally different ways: in FAST, wind profiles are created using TurbSim, while SOWFA requires precursor simulations to generate turbulent wind conditions. As such, the wind profiles, shown in Fig. 8 cannot be compared directly. However, the mean wind speed and TI can be compared. The TI I is defined as

$$I = \frac{\sigma_U}{\mu_U}, \tag{6}$$

where μ_U and σ_U are the mean value and standard deviation, respectively, of the wind U as shown in Fig. 8.

The mean wind speed and TI for both simulation tools are shown in Table 3. It is concluded from these results that an additional effort is desired to improve the similarity between flow fields in FAST and SOWFA. Although the flow fields from the simulations presented here are not identical, they are similar enough to permit a first comparison between the simulations performed in FAST and SOWFA, and thus enable evaluation of the loads on a downstream turbine.

Next, the turbine performance is compared. The most important signals of the wind turbine are shown in Fig. 9. This figure shows that the generator torque and rotor speed are slightly higher in SOWFA. As a result, the power production in SOWFA is also higher. For the blade and tower moments, it can be observed that, in FAST, the variations of these signals are larger. This can partly be explained by the way the turbine is modeled in SOWFA: the ALM implementation does not model the tower dynamics. As a result, the vibrations caused by the natural frequency of the tower (which is 0.324 Hz [24]) are not present in the SOWFA tower moments. This is clearly visible in Fig. 10: in FAST, a clear peak is visible at this natural frequency that is absent in SOWFA. As a result, the Damage Equivalent Load (DEL) of the tower is expected to be higher in FAST than in SOWFA. The power spectrum of the blade OoP bending moments show better resemblance between FAST and SOWFA, with only a slightly higher peak at the once-per-revolution (1P) frequency in FAST. Subsequently, the DELs of the blade moments are expected to be similar in FAST and SOWFA.

A similar analysis can be made for the different wake mixing strategies defined in Section 4: Dynamic Induction Control (DIC), helix counterclockwise (CCW) and helix clockwise (CW). For the sake of clarity, the tower moments power spectra from SOWFA are omitted in these analyses, as the effect of the control strategies is very similar in both simulation tools.

Table 4 summarizes the DELs for the turbine blades and tower in both FAST and SOWFA. What stands out in this comparison is that SOWFA overestimates the increase in blade DELs when wake mixing strategies are applied, while it underestimates the tower DEL. The former can be explained by a relatively lower baseline DEL, while the latter is influenced by the lack of a tower model in SOWFA. While there is a clear discrepency between the DELs obtained from the different tools, the load signals, specifically of the blades, are similar enough to justify an analysis of the loads on the downstream turbine in SOWFA. This analysis is executed in Section 5.3.

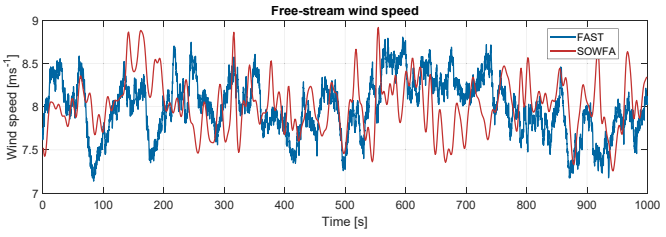

Fig. 8. Development of the free-stream wind speed over the run time of 1000 s in the different simulation tools: FAST and SOWFA.

5.3. Downstream turbine loads

Using the Computational Fluid Dynamics (CFD) simulations from SOWFA, the loads experienced by a downstream turbine can be evaluated. As described in Section 2, a second turbine (T2) is placed at 5 rotor diameters (5D) downstream of the controlled turbine. This turbine is controlled using steady-state greedy control, *i.e.* the same control as the baseline case for turbine 1. In this section, the loads experienced by this machine, as obtained from SOWFA, are evaluated. These simulations are identical to the SOWFA simulations presented in Section 5.2, but this time with a second turbine in the wake of the controlled turbine.

Fig. 11 shows the different output signals of T2 over time, when the different wake mixing strategies are implemented on the upstream turbine (T1). Compared to Fig. 9, it can be observed that, due to the lower wind speed in the wake, the average rotor thrust is also lower. Subsequently, also the average blade and tower bending moments are lower. However, the fluctuations of these signals are significantly larger, which is expected to result in a higher DEL.

The power spectral densities of the blade and tower bending moments are depicted in Fig. 12. This figure confirms that although the steady-state moments are lower, the power over the entire frequency spectrum increases. The PSD still exhibits the peaks that are inherent to normal turbine operation: at 1P, 2P and 3P for the blades and at 3P for the tower. Furthermore, when DIC is applied on T1, this also results in a clear peak at T2: not only at the excitation frequency f_e, but also at multiple $2f_e$. The sinusoidal thrust force at T1 results in peaks in the wind speed spectrum at f_e and its multiples (with decreasing amplitude), which is propagated to the loads on T2. For the helix, the variations of the wind speed in the wake over time are much less significant, and as a result, these peaks are not or barely present there. Small peaks are visible at the pitch frequency, close to 1P, but these peaks are much smaller than at T1. In general, the PSD of the bending moments at T2 are much more similar to the baseline case.

The DEL of these moments is calculated for the second turbine, and listed in Table 5. The results show that the DELs on the second turbine are in general higher than on T1, also when no wake mixing is implemented. Furthermore, the different dynamic wake mixing strategies applied on the first turbine also increase the loads on the second turbine with respect to baseline greedy control on T1. This is to be expected, as these strategies increase both the average wind speed and the variation of wind speed in the wake. To compare the benefit of wake mixing strategies in terms of power production with the disadvantage of increased loads, the relative power production of the downstream turbines with respect to baseline is also given in the table. For more details on the increased power production that can be achieved with these strategies, the reader is referred to Ref. [20].

A comparison between the different wake mixing strategies shows that the helix results in lower DELs on the downstream turbine than DIC. This can be explained by how the helix works: the rotation of the wake increases wake mixing with limited variations in the induction of T1. Subsequently, it generates less variations in wind speed in the wake than DIC, and the downstream turbine therefore experiences lower DELs.

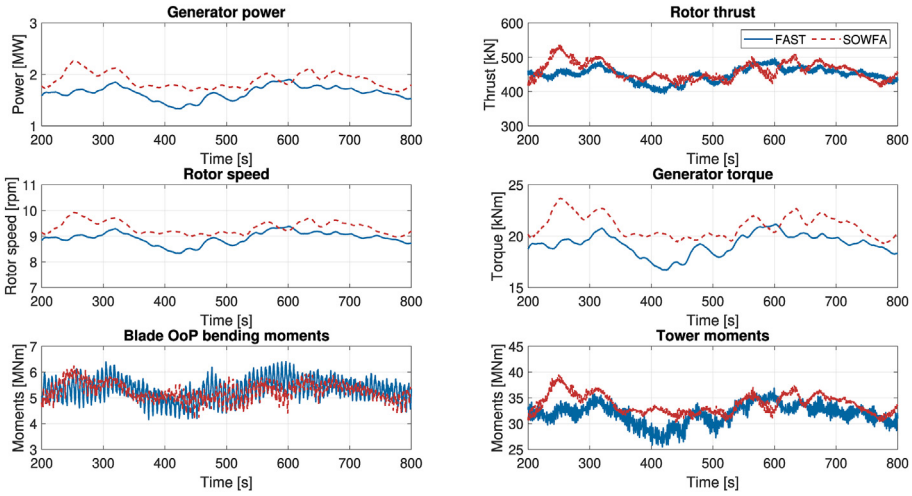

Fig. 9. The evolution of the power and load-related signals of the turbine in FAST (solid blue) and SOWFA (dashed red), for an inflow wind speed of 8 ms^{-1} and a turbulence intensity of around 5%.

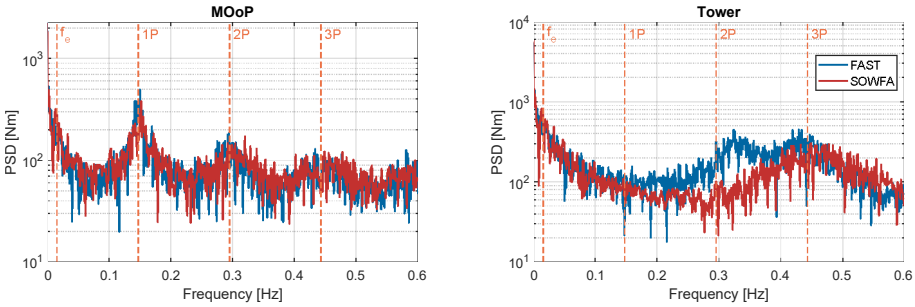

Fig. 10. The Power Spectral Density (PSD) of the blade Moments Out-of-Plane (MOoP, left) and the tower moments (right) for the simulations with baseline greedy control applied on the turbines in FAST and SOWFA, as described above.

The DELs of the blades are in all cases significantly lower than the DELs of the controlled turbine. This is to be expected, as the blades of this turbine are not actively pitched to enhance wake mixing. The tower loads are lower that on T1 for DIC, while they are higher for the helix. Nonetheless, both helix strategies result in a lower tower DEL than DIC.

Based on the results presented in Table 5, it can be concluded that the effect of wake mixing strategies on the loads of a downstream turbine is less significant than on the upstream machine. Furthermore, when only taking into account the DELs on downstream turbine, the helix approach should be the preferred wake mixing strategy compared to DIC.

5.4. Pitch bearing damage

Apart from imposing an additional load on the turbine itself, the pitch actuation required for dynamic wake mixing strategies also increases the chance of pitch bearing damage. In this section, the consequences of this increased actuation on the bearings is evaluated for the different wake mixing strategies. As a comparison, a classical Individual Pitch Control (IPC) for load alleviation case is chosen, as described in Section 4. This control approach requires similar pitch actuation as the helix, and can therefore serve as a frame of reference. To quantify the risk of bearing damage, the methodology outlined in Section 3.2 is used.

Fig. 13 shows the relevant signals for the analysis of the pitch bearings for a representative section of the simulation. For the sake of clarity, the clockwise (CW) helix approach is omitted here. From this figure, it follows that the IPC pitch actuation has a smaller amplitude than with the wake mixing strategy. As demonstrated in Section 4, the frequency is also slightly lower than the frequency of the counterclockwise (CCW) helix. The corresponding blade bending moments for the wake mixing strategies exhibit much larger oscillations than with IPC. It should be noted however that for the pitch bearing damage, unlike with the turbine fatigue loads, the absolute value of the load over a cycle is evaluated. Larger variations in these loads do therefore not necessarily lead to a higher likelihood of pitch bearing damage occurring.

The cycle count obtained with range-pair counting for the different control algorithms in the below-rated regime (8 ms^{-1}) and low TI are given in Table 6. In these conditions, the cycles are straightforward: all oscillations originate from the dynamic controller, as the baseline controller prescribes no pitching. As a result, all cycles have the same amplitude for the wake mixing strategies. For IPC, the cycles are divided over two bins, as the average amplitude with IPC is approximately 3°. The few single cycles with a smaller amplitude can be explained by incomplete cycles at the beginning or the end of the simulation.

From Table 6, it can be concluded that the helix results in a significant increase in load cycles, although only slightly more than conventional IPC. A factor that increases the risk of surface-induced damage, is the fact that all oscillations are around the mean value of 0°. However, the amplitude of these oscillations, 5°, is relatively big. This decreases the risk of surface-induced damage, as the contact area on the bearing raceway is relatively large [33].

From Table 6, it can be concluded that the oscillating cycles that

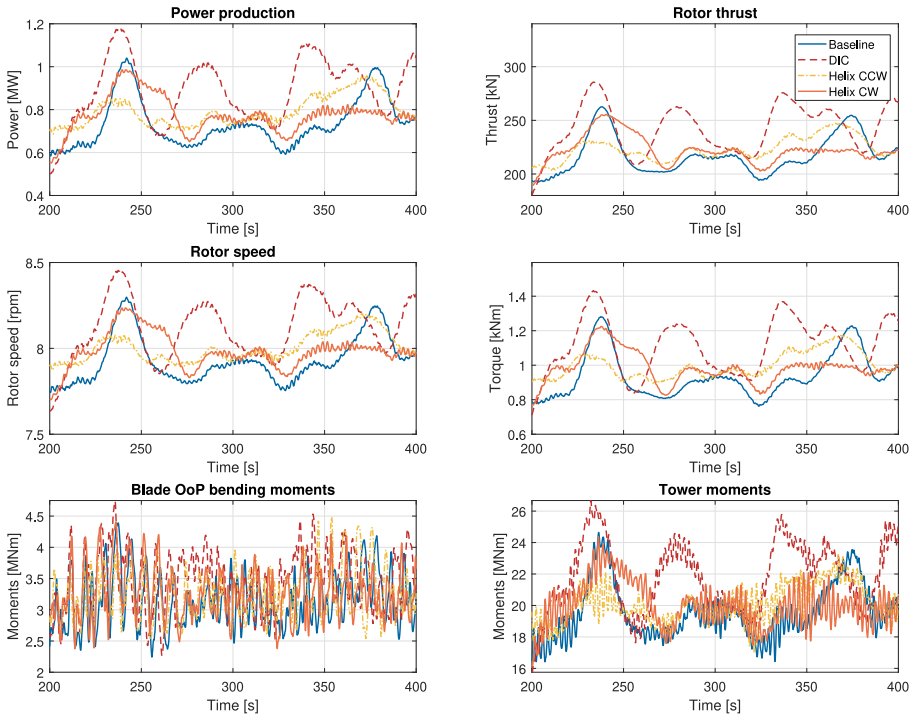

Fig. 11. The evolution of the power and load-related signals of the downstream turbine (T2) in SOWFA, when different control strategies are implemented on the upstream turbine (T1). The simulations are executed with an inflow wind speed of 8 ms^{-1} and a turbulence intensity of around 5%.

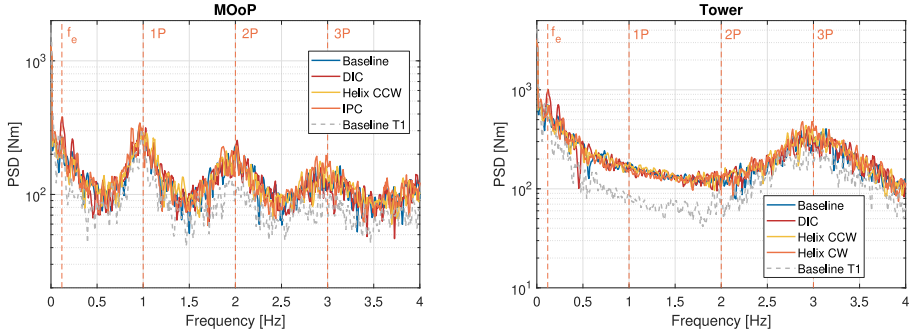

Fig. 12. The Power Spectral Density (PSD) of the blade Out-of-Plane (OoP, left) and tower (right) bending moments of T2, when different wake mixing strategies are implemented on T1. As comparison, the PSD of T1 with baseline operation is shown in grey. The frequency is normalized with respect to the turbine rotor speed to enable a comparison between T1 and T2.

Table 5
Damage Equivalent Load (DEL) results for a downstream turbine, when located in the wake of a turbine executing different control strategies. All percentages shown are relative to the corresponding baseline case. For comparison, the relative power production gained is also shown.

	Baseline	DIC	Helix CCW	Helix CW
Blades (SOWFA) [Nm]	$2.83 \cdot 10^6$	$3.30 \cdot 10^6$	$3.05 \cdot 10^6$	$3.20 \cdot 10^6$
W.r.t. Baseline		+16.8%	+8.0%	+13.3%
W.r.t. Baseline T1	+20.5%	+40.8%	+30.1%	+36.6%
Tower (SOWFA) [Nm]	$1.14 \cdot 10^7$	$1.46 \cdot 10^7$	$1.40 \cdot 10^7$	$1.30 \cdot 10^7$
W.r.t. Baseline		+27.9%	+22.2%	+13.4%
W.r.t. Baseline T1	+3.5%	+32.4%	+26.5%	+17.4%
Power w.r.t. Baseline		+4.6%	+12.1%	+5.4%

a pitch bearing has to endure with the helix approach, are on itself no more harmful than with conventional IPC. Next, the magnitude of the load on the bearings during these cycles is identified. To achieve this, the bending moments on the blades during these cycles are divided into bins. Fig. 14a shows the percentage of operating time that each load bin contributes to the overall cycle time. The variations in the load that is visible for the wake mixing strategies in Fig. 13, can also be seen here. 82% of the operating time in spent in the 5–6 MNm bin when IPC is applied, while with the wake mixing strategies, the loads are more evenly distributed over a range of 4–7 MNm.

By combining the results of Table 6 and Fig. 14a, the risk of fatigue damage on the pitch bearings can be assessed. These results show that in below-rated wind conditions, with a relatively low TI of 5%, the dynamic wake mixing strategies do not pose a significant increased risk of pitch bearing damage compared to conventional IPC. Neither the amount of cycles, nor the resulting bending moments during these cycles is significantly higher when the helix approach is implemented. With DIC, the amount of cycles is a factor 10 lower than with IPC, while the resulting bending moments are

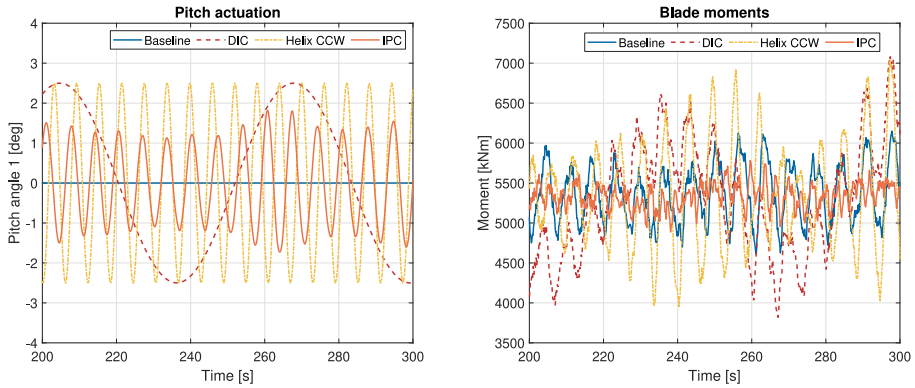

Fig. 13. The pitch actuation (left) and bending moments (right) for blade 1 of the turbine, obtained from simulations in FAST for different control strategies. The operating regime is below-rated with an average wind velocity of 8 ms^{-1} and an average turbulence intensity of 5%.

Table 6
Results of the cycle count in low TI, below-rated wind conditions.

Amplitude (°)	IPC	DIC	Helix CCW	Helix CW
0–0.4	1	0	0	1
0.4–1	1	1	2	1
1–3	202	1	0	1
3–7	63	28	295	237
7–15	0	0	0	0

Table 7
Results of the cycle count in high TI, below-rated wind conditions.

Amplitude (°)	IPC	DIC	Helix CCW	Helix CW
0–0.4	19	0	0	39
0.4–1	20	1	2	3
1–3	98	1	0	0
3–7	147	28	308	251
7–15	23	0	0	0

comparable. It can therefore be concluded that, in these conditions, DIC poses very little risk of pitch bearing damage, while the helix approach poses a risk that is similar to conventional IPC.

The case evaluated above is the most relevant in terms of the application of wake mixing strategies. However, from a pitch actuation point of view, it is also the most straightforward case. For the sake of completeness, a case with higher turbulence is also evaluated, both in the below-rated (8 ms^{-1}) and above-rated (14 ms^{-1}) regime. The results of the former simulations are summarized in Table 7. Comparing these results with the low TI results shown in Table 6, it becomes clear that the higher turbulence has limited influence on the load cycles of the different control strategies. The turbulent inflow results in slightly more variations of the cycle amplitudes, but the number of cycles and the dominant amplitudes stay more or less the same. In these conditions, the risk of pitch bearing damage of DIC is still very small, while the helix and conventional IPC result in a similar load cycle pattern.

Fig. 14b shows the load bins for the different control strategies when applied in below-rated, high TI wind conditions. Comparing to the low TI results, it can be observed that the loads vary more and over a wider range of magnitudes. Where Fig. 14a shows that IPC is very effective in keeping the blade load variations minimal, it is clearly less effective in turbulent wind conditions. The difference between IPC and the wake mixing strategies is much smaller in these conditions, as the turbulent wind accounts for a significant amount of the load variations measured here.

In above-rated wind conditions, the pitch actuation is a summation of the baseline control aimed at keeping the power output constant, and the periodic signal from IPC or wake mixing control. The resulting pitch and load signals for a segment of these simulations are shown in Fig. 15. This figure clearly shows the baseline pitch control for power regulation superimposed on the periodic signals from the different control strategies. As a result, the cycles are also more evenly distributed among different amplitude bins. This is shown in Table 8.

Compared to Table 6, some of the cycles have shifted to the lower-amplitude bins, specifically for conventional IPC. However, the dominant cyclic behavior of the controller is clearly visible; the

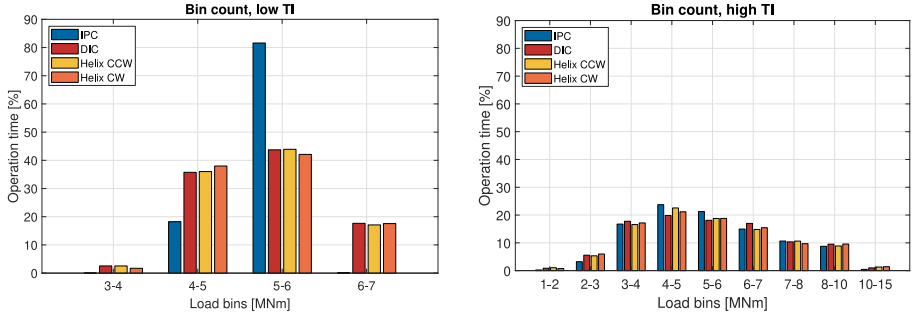

(a) Results of low TI (5 %) free-stream wind. (b) Results of high TI (16 %) free-stream wind.

Fig. 14. The percentage of operating time spent in each load bin during the dominant oscillation cycles of different control strategies operating in below-rated wind conditions. The results in low TI are shown on the left, the results in high TI on the right.
(a) Results of low TI (5%) free-stream wind.
(b) Results of high TI (16%) free-stream wind.

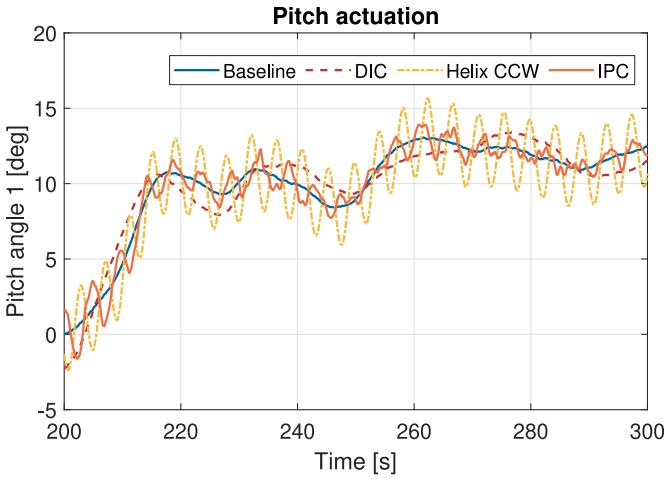

Fig. 15. The pitch actuation for blade 1 of the turbine, obtained from simulations in FAST for different control strategies. The operating regime is below-rated with an average wind velocity of 14 ms^{-1} and an average turbulence intensity of 16%.

bins that contain the amplitude of the prescribed pitch motion still counts the largest amount of cycles. Recall that oscillations with a smaller amplitude are in general more likely to cause fatigue damage to the bearing raceway. These oscillations with a very small amplitude continue to be minimal for the wake mixing strategies.

Contrary to the below-rated case, the mean pitch value around which the oscillations occur is not necessarily always zero. Due to the varying pitch angle prescribed by the baseline controller, the affected location on the raceway of the bearing varies over time, see Fig. 16a. Subsequently, the stress on the bearing is also distributed over a larger part of the raceway, which reduces the risk of fatigue damage to the bearing.

Due to the higher wind speed and increased turbulence, the variations in the blade bending moments are also larger. This is shown in Fig. 16b, where the last bin now runs up to 14 MNm. Similar to the low-TI, below-rated case, the variations of the loads are lower with IPC. However, in general it can be concluded that the loads on the bearing are very similar in magnitude.

To conclude, the results presented in this section provide a number of beneficial circumstances when looking at the blade bearings. First of all, the amplitudes of the dominant oscillations are relatively large, whereas bearing damage is more likely to occur when this amplitude is very small. Secondly, the average load on the bearings does not increase significantly compared to conventional IPC. Finally, the loads on the bearing do increase as wind speed and turbulence intensity increases. However, at above-rated wind speeds, the average pitch angle around which the oscillations occur, varies over time. As a result, the stress is distributed over a larger part of the bearing raceway, reducing the risk of fatigue damage. These results together suggest that the dynamic wake mixing strategies presented in this paper are unlikely to significantly increase the risk of blade bearing fatigue damage.

Table 8
Results of the cycle count in high TI, above-rated wind conditions.

Amplitude (°)	IPC	DIC	Helix CCW	Helix CW
0–0.4	30	5	4	8
0.4–1	36	7	9	3
1–3	124	12	58	37
3–7	61	21	231	246
7–15	4	14	1	0

6. Conclusions

In different recent studies, strategies that use pitch control to enhance wake mixing have been assessed. The results of these studies show that such strategies can be extremely effective when it comes to increasing wind farm power production. At the same time, the increased pitch actuation of these strategies raised questions on the implementability, as a thorough analysis of the effects on the fatigue loads of different critical turbine components was lacking.

In this paper, a turbine load analysis is presented for different active wake mixing strategies, based on simulations in the well-known codes FAST and SOWFA. The Damage Equivalent Load (DEL) of critical components such as the blades and the tower are compared, and the risk of fatigue damage to the blade bearings is assessed. The wake mixing approaches that are evaluated here are Dynamic Induction Control (DIC), where the collective pitch angle is varied slowly, and the helix approach, where the individual pitch angles are used to create time-varying tilt and yaw moments. Both methods have shown in literature to improve wind farm power capture by several percent.

The results presented in this paper show that, as expected, these wake mixing strategies increase the DEL on the blades and tower of the turbine. In general, DIC has a very high impact on the tower of the controlled turbine, increasing the DEL by up to a factor 2. The helix approach has a much smaller impact on the tower, with a maximal increase in DEL of 11.4%. For the blades, the opposite holds: as the helix approach requires pitch actuation at a much higher rate, the blade loads are also affected more by this strategy. However, for below-rated wind conditions, in which wake mixing is the most relevant, the difference in blade loads between DIC and the helix approach is minimal.

Using flow simulations in the high-fidelity flow model SOWFA, the turbine loads of a downstream turbine are also estimated. These simulations show that an additional effort is needed to make the flow fields in FAST and SOWFA more comparable. Nevertheless, the simulations indicate that all wake mixing strategies increase both the blade and tower DEL of a downstream turbine. DIC clearly has the most severe effect, performing 5–10% worse than the helix approach in terms of turbine DELs. Nonetheless, the most extreme increase in DEL is observed at the upstream turbine rather than the downstream machine.

Finally, an analysis on the risk of pitch bearing damage is executed. From this analysis, it follows that the amount of oscillations with a very small amplitude are limited with all wake mixing strategies, and the average loads are of the same order of magnitude as with a comparison case of conventional Individual Pitch Control (IPC). In above-rated, higher turbulent conditions, the number of cycles and the average loads increase. At the same time, the average pitch angle around which the cycles occur also changes, which in turn decreases the risk of fatigue damage to the bearings. As a result, it can be concluded that wake mixing strategies using IPC have limited effect on the risk of fatigue damage to the pitch bearings. The results show that this risk is similar to or smaller than when conventional IPC is implemented.

Although the results presented here are promising, it as of yet too soon to draw a definitive conclusion on the implementability of dynamic wake mixing strategies such as DIC or the helix approach. The next step in validating the results presented here would be to execute a measurement campaign on full-scale wind turbines to assess the damage equivalent load in real-world conditions.

To conclude, different aspects of turbine fatigue damage due to wake mixing strategies have been investigated in this paper. The helix approach has a less beneficial effect on the blades, while DIC impacts the turbine tower more. The increased risk of fatigue

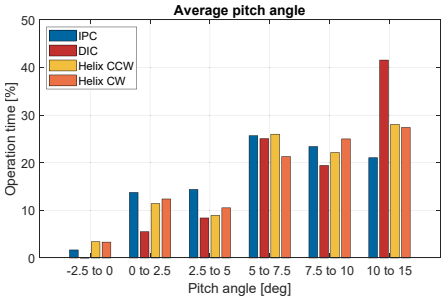

(a) Bins of the mean pitch angle during the dominant oscillations, for the high TI, above-rated wind conditions.

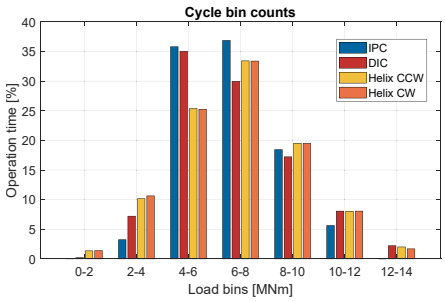

(b) Bins of the bending moment during the dominant oscillations, for the high TI, above-rated wind conditions.

Fig. 16. Bin counts in percentages of the operation time during oscillations. On the left, the pitch angle around which the dominant oscillations occur are binned. On the right, the same is done with the load on the bearings during these oscillations.
(a) Bins of the mean pitch angle during the dominant oscillations, for the high TI, above-rated wind conditions.
(b) Bins of the bending moment during the dominant oscillations, for the high TI, above-rated wind conditions.

damage on the blade bearings is assessed as minimal. Although the increased pitch actuation and associated variations in turbine loads are undeniable, the consequences are not so severe as to disqualify dynamic wake mixing as a wind farm control strategy. The results presented in this paper therefore support the proposition that wake mixing approaches such as DIC and the helix approach can be valuable control strategies in the wind farms of the future, and require further investigation to determine their full potential.

CRediT authorship contribution statement

Joeri A. Frederik: Conceptualization, Methodology, Validation, Investigation, Writing – original draft, Visualization. **Jan-Willem van Wingerden:** Conceptualization, Writing – review & editing, Supervision.

Declaration of competing interest

The authors declare that they have no known competing financial interests or personal relationships that could have appeared to influence the work reported in this paper.

References

[1] N. Panwar, S. Kaushik, S. Kothari, Role of renewable energy sources in environmental protection: a review, Renew. Sustain. Energy Rev. 15 (3) (2011) 1513–1524, https://doi.org/10.1016/j.rser.2010.11.037.
[2] Dnv-GL, Energy transition outlook, Tech. Rep. (2020).
[3] Klimaatakkoord Rijksoverheid, Tech. Rep. (2019). URL, https://www.rijksoverheid.nl/binaries/rijksoverheid/documenten/rapporten/2019/06/28/klimaatakkoord/klimaatakkoord.pdf.
[4] S. Boersma, B. Doekemeijer, P.M. Gebraad, P.A. Fleming, J. Annoni, A.K. Scholbrock, J.A. Frederik, J.W. van Wingerden, A tutorial on control-oriented modeling and control of wind farms, in: 2017 American Control Conference (ACC), 2017, pp. 1–18, https://doi.org/10.23919/ACC.2017.7962923.
[5] M.A. Rotea, Dynamic programming framework for wind power maximization, IFAC Proc. Vol. 47 (3) (2014) 3639–3644, https://doi.org/10.3182/20140824-6-ZA-1003.02071.
[6] J. Annoni, P.M. Gebraad, A.K. Scholbrock, P.A. Fleming, J.W. van Wingerden, Analysis of axial-induction-based wind plant control using an engineering and a high-order wind plant model, Wind Energy 19 (6) (2016) 1135–1150, https://doi.org/10.1002/we.1891.
[7] F. Campagnolo, V. Petrović, C.L. Bottasso, A. Croce, Wind tunnel testing of wake control strategies, in: 2016 American Control Conference, ACC), 2016, pp. 513–518, https://doi.org/10.1109/acc.2016.7524965.
[8] P. Fleming, J. Annoni, J.J. Shah, L. Wang, S. Ananthan, Z. Zhang, K. Hutchings, P. Wang, W. Chen, L. Chen, Field test of wake steering at an offshore wind farm, Wind Energy Sci. 2 (1) (2017) 229–239, https://doi.org/10.5194/wes-2-229-2017.
[9] Á. Jiménez, A. Crespo, E. Migoya, Application of a les technique to characterize the wake deflection of a wind turbine in yaw, Wind Energy 13 (6) (2010) 559–572, https://doi.org/10.1002/we.380.
[10] M. Bastankhah, F. Porté-Agel, Experimental and theoretical study of wind turbine wakes in yawed conditions, J. Fluid Mech. 806 (2016) 506–541, https://doi.org/10.1017/jfm.2016.595.
[11] F. Campagnolo, V. Petrović, E. Nanos, C. Tan, C. Bottasso, H. K. I. Paek, K. Kim, Wind tunnel testing of power maximization control strategies applied to a multi-turbine floating wind power platform, Proceedings of the International Offshore and Polar Engineering Conference.
[12] P. Fleming, J. King, K. Dykes, E. Simley, J. Roadman, A. Scholbrock, P. Murphy, J. K. Lundquist, P. Moriarty, K. Fleming, et al., Initial results from a field campaign of wake steering applied at a commercial wind farm–part 1, Wind Energy Sci. 4 (NREL/JA-5000-73991). doi:10.5194/wes-4-273-2019.
[13] P. Fleming, J. King, E. Simley, J. Roadman, A. Scholbrock, P. Murphy, J.K. Lundquist, P. Moriarty, K. Fleming, J.v. Dam, et al., Continued results from a field campaign of wake steering applied at a commercial wind farm–part 2, Wind Energy Sci. 5 (3) (2020) 945–958, https://doi.org/10.5194/wes-5-945-2020.
[14] B. M. Doekemeijer, S. Kern, S. Maturu, S. Kanev, B. Salbert, J. Schreiber, F. Campagnolo, C. L. Bottasso, S. Schuler, F. Wilts, et al., Field Experiment for Open-Loop Yaw-Based Wake Steering at a Commercial Onshore Wind Farm in italy, Wind Energy Science Discussionsdoi:10.5194/wes-2020-80.
[15] J.P. Goit, J. Meyers, Optimal control of energy extraction in wind-farm boundary layers, J. Fluid Mech. 768 (2015) 5–50, https://doi.org/10.1017/jfm.2015.70.
[16] W. Munters, J. Meyers, Towards practical dynamic induction control of wind farms: analysis of optimally controlled wind-farm boundary layers and sinusoidal induction control of first-row turbines, Wind Energy Sci. 3 (1) (2018) 409–425, https://doi.org/10.5194/wes-3-409-2018.
[17] J.A. Frederik, R. Weber, S. Cacciola, F. Campagnolo, A. Croce, C. Bottasso, J.W. van Wingerden, et al., Periodic dynamic induction control of wind farms: proving the potential in simulations and wind tunnel experiments, Wind Energy Sci. 5 (1) (2020) 245–257, https://doi.org/10.5194/wes-5-245-2020.
[18] W. Munters, J. Meyers, Dynamic strategies for yaw and induction control of wind farms based on large-eddy simulation and optimization, Energies 11 (1) (2018) 177, https://doi.org/10.3390/en11010177.
[19] K. Kimura, Y. Tanabe, Y. Matsuo, M. Iida, Forced wake meandering for rapid recovery of velocity deficits in a wind turbine wake, in: AIAA Scitech 2019 Forum, 2019, p. 2083, https://doi.org/10.2514/6.2019-2083.
[20] J. A. Frederik, B. M. Doekemeijer, S. P. Mulders, J. W. van Wingerden, The Helix Approach: Using Dynamic Individual Pitch Control to Enhance Wake Mixing in Wind Farms, Wind Energy.
[21] NWTC, Openfast, URL, http://openfast.readthedocs.io, 2018.
[22] J.M. Jonkman, L.J. Buhl, Marshall, Fast user's guide, in: Tech. Rep. NREL/EL-500-38230, National Renewable Energy Laboratory (NREL), 15013 Denver West Parkway, Golden, CO, 2005. https://nwtc.nrel.gov/FAST.
[23] M. Churchfield, S. Lee, Nwtc design codes – sowfa, in: Tech. Rep, National Renewable Energy Laboratory (NREL), 2012. URL, http://wind.nrel.gov/designcodes/simulators/SOWFA.
[24] J.M. Jonkman, S. Butterfield, W. Musial, G. Scott, Definition of a 5-mw reference wind turbine for offshore system development, in: Tech. Rep. NREL/TP-500-38060, National Renewable Energy Laboratory (NREL), 2009.
[25] IEC 61400-1, Wind turbines — part 1: design requirements, in: Tech. Rep, Garrad Hassan and Partners Ltd, 2004.
[26] J.A. Frederik, B.M. Doekemeijer, S.P. Mulders, J.W. van Wingerden, On wind farm wake mixing strategies using dynamic individual pitch control, in: Journal of Physics: Conference Series, 1618, IOP Publishing, 2020, p. 22050.
[27] T.-S. Leu, J.-M. Yo, Y.-T. Tsai, J.-J. Miau, T.-C. Wang, C.-C. Tseng, Assessment of iec 61400-1 normal turbulence model for wind conditions in taiwan west coast areas, in: International Journal of Modern Physics: Conference Series, 34, World Scientific, 2014, p. 1460382.

[28] J.N. Sørensen, W.Z. Shen, Numerical modeling of wind turbine wakes, J. Fluid Eng. 124 (2) (2002) 393–399, https://doi.org/10.1115/1.1471361.
[29] E.A. Bossanyi, Individual blade pitch control for load reduction, Wind Energy 6 (2) (2003) 119–128, https://doi.org/10.1002/we.76.
[30] K. Thomsen, P. Sørensen, Fatigue loads for wind turbines operating in wakes, J. Wind Eng. Ind. Aerod. 80 (1–2) (1999) 121–136.
[31] S. Lee, M. Churchfield, F. Driscoll, S. Sirnivas, J. Jonkman, P. Moriarty, B. Skaare, F.G. Nielsen, E. Byklum, Load estimation of offshore wind turbines, Energies 11 (7) (2018) 1895.
[32] D. Pérez-Campuzano, E. Gómez de las Heras-Carbonell, C. Gallego-Castillo, A. Cuerva, Modelling damage equivalent loads in wind turbines from general operational signals: exploration of relevant input selection methods using aeroelastic simulations, Wind Energy 21 (6) (2018) 441–459.
[33] M. Stammler, A. Reuter, G. Poll, Cycle counting of roller bearing oscillations–case study of wind turbine individual pitching system, Renew. Energy Focus 25 (2018) 40–47.
[34] M. Stammler, P. Thomas, A. Reuter, F. Schwack, G. Poll, Effect of load reduction mechanisms on loads and blade bearing movements of wind turbines, Wind Energy 23 (2) (2020) 274–290.
[35] M. Stammler, G. Poll, Schadensmechanismen in rotorblattlagern, GfT-Reibung, Schmierung und Verschleiss, Göttingen (2014).
[36] E. Bossanyi, The design of closed loop controllers for wind turbines, Wind Energy 3 (3) (2000) 149–163, https://doi.org/10.1002/we.34.
[37] S.P. Mulders, T.G. Hovgaard, J.D. Grunnet, J.-W. van Wingerden, Preventing wind turbine tower natural frequency excitation with a quasi-lpv model predictive control scheme, Wind Energy 23 (3) (2020) 627–644.
[38] E.A. Bossanyi, Further load reductions with individual pitch control, Wind Energy 8 (4) (2005) 481–485, https://doi.org/10.1002/we.166.
[39] G. Bir, Multi-blade coordinate transformation and its application to wind turbine analysis, in: 46th AIAA Aerospace Sciences Meeting and Exhibit, 2008, p. 1300, https://doi.org/10.2514/6.2008-1300.
[40] S.P. Mulders, A.K. Pamososuryo, G.E. Disario, J.W. van Wingerden, Analysis and optimal individual pitch control decoupling by inclusion of an azimuth offset in the multiblade coordinate transformation, Wind Energy 22 (3) (2019) 341–359, https://doi.org/10.1002/we.2289.
[41] P.A. Fleming, P.M. Gebraad, S. Lee, J.W. van Wingerden, K. Johnson, M. Churchfield, J. Michalakes, P. Spalart, P. Moriarty, Evaluating techniques for redirecting turbine wakes using sowfa, Renew. Energy 70 (2014) 211–218, https://doi.org/10.1016/j.renene.2014.02.015.
[42] C.L. Bottasso, A. Croce, Cp-lambda User Manual, Tech. Rep, Dipartimento di Scienze e Tecnologie Aerospaziali, Politecnico di Milano, Milano, Italy, 2009.